Chem Biol Drug Des 2013; **82:** 351–360

Research Letter

Synthesis and *in vitro* Evaluation of 1,2,4-Triazolo[1,5-*a*][1,3,5]triazine Derivatives as Thymidine Phosphorylase Inhibitors

Hriday Bera[1,2,*], Anton V. Dolzhenko[2,3], Lingyi Sun[2], Sayan Dutta Gupta[1] and Wai-Keung Chui[2,*]

[1]*Gokaraju Rangaraju College of Pharmacy, Bachupally, Hyderabad 500090, India*
[2]*Department of Pharmacy, Faculty of Science, National University of Singapore, 18 Science Drive 4, Singapore 117543, Singapore*
[3]*School of Pharmacy, Monash University Sunway Campus, Jalan Lagoon Selatan, Bandar Sunway, Selangor, WA-46150, Malaysia*
**Corresponding authors: Hriday Bera, hriday.bera@gmail.com; Wai-Keung Chui, phacwk@nus.edu.sg*

In our lead finding program, a series of 1,2,4-triazolo [1,5-*a*][1,3,5]triazine derivatives were synthesized, and their *in vitro* thymidine phosphorylase inhibitory potential was explored. Among the different derivatives, compounds having keto group (C = O) at C7 and thioketo group (C = S) at C5 positions showed varying degrees of TP inhibitory activity comparable with positive control, 7-deazaxanthine (7-DX, 2) (IC_{50} value = 42.63 μM). Enzyme inhibition kinetics study suggested that compound IVn behaved as a mixed-type inhibitor of the enzyme with respect to thymidine (dThd) as a variable substrate. Compound IVn was also found to inhibit PMA-induced MMP-9 expression in MDA-MB-231 cells at sublethal concentrations. Computational docking study was performed to illustrate the enzyme inhibition kinetics and to explore the ligand–enzyme interactions.

Key words: 1,2,4-triazolo[1,5-*a*][1,3,5]triazine, computational docking study, intramolecular heterocyclization, mixed-type inhibition, thymidine phosphorylase inhibitors

Received 30 March 2013, revised 15 May 2013 and accepted for publication 6 June 2013

Introduction

Thymidine phosphorylase (TP, EC 2.4.2.4), also known as platelet-derived endothelial cell growth factor (PD-ECGF) and gliostatin (1), catalyses the reversible phosphorolysis of thymidine or 2'-deoxyuridine and their analogues into 2-deoxy-alpha-D-ribose-1-phosphate (2DDR-1P) and the respective bases (2). It also acts in the salvage pathway of pyrimidine nucleotides by transferring the deoxyribosyl moiety to form new nucleoside (3). TP is overexpressed in many solid tumors (4), including esophageal, gastric, pancreatic, ovarian, breast, renal, bladder and non-small-cell lung cancers (5,6). It is reported that this enzyme and its metabolite, 2DDR-1P, stimulate the secretion and/or expression of the angiogenic agents, including metalloproteases and other matrix-degrading enzymes (MMPs), and induce endothelial cell migration (7–11). In addition, increased level of TP is associated with protection of the tumor against apoptosis (12,13) and enhancement of metastatic potential (14) that may influence tumor progression (15). Therefore, inhibition of thymidine phosphorylase may be viewed as a plausible strategy to overcome its pathological effects. In addition, TP inhibitors may also serve as adjuvant to enhance the bioavailability and therapeutic efficacy of coadministered anticancer drugs that belong to the deoxynucleosides (16).

Pioneering works in this field generated several potent thymidine phosphorylase inhibitors (6,17,18), most of these inhibitors are derivatives of pyrimidine-2,4-dione with only a few that are fused bicyclic heterocycles possessing the homophthalimide moiety, which is believed to be essential for binding to the active site of this enzyme (19). Fukushima *et al.* (20) synthesized 5-chloro-6-[1-(2-iminopyrrolidinyl) methyl] uracil hydrochloride (**TPI**, **1**) (Figure 1), the most potent human TP inhibitor known so far, which has an IC_{50} value of 35 nM and K_i of 20 nM.

Derivatives of 1,2,4-triazolo[1,5-*a*][1,3,5]triazine have shown various bioactivities such as selective adenosine receptor antagonism (21,22) and xanthine oxidase inhibition (23). Besides these activities, this scaffold also exhibits anti-inflammatory, antioxidant, antiproliferative, antibacterial and antifungal properties (24). However, inhibitory activity of this fused heterobicyclic system against TP has not yet been explored. It is hypothesized that structural modifications of 7-deazaxanthine (**7-DX**, **2**) (Figure 1), a bicyclic lead compound, by replacing two carbons at positions C9 and C5 with nitrogen moiety and inserting various substitutions at position C6 would demonstrate TP inhibitory activity. To test this hypothesis, a series of 1,2,4-triazolo[1,5-*a*][1,3,5]triazines (Figure 2) were synthesized *via* a practical

 doi: 10.1111/cbdd.12171

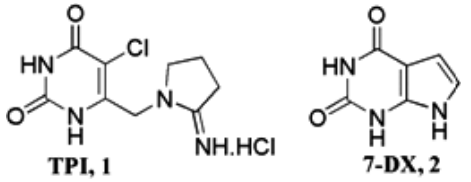

Figure 1: Structures of known TP inhibitors.

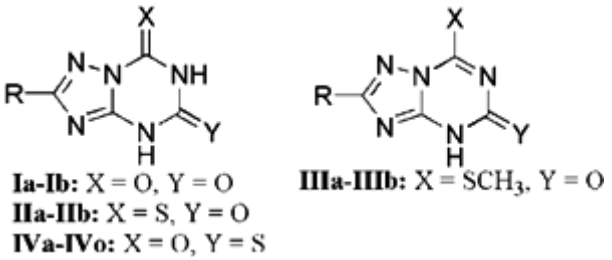

Figure 2: Structures of synthesized 1,2,4-triazolo[1,5-*a*][1,3,5] triazine.

synthetic approach, and the target compounds were evaluated for TP inhibition using an *in vitro* enzyme assay. To investigate the pharmacophoric requirements and explore the chemical space of the active site of the enzyme, positions C5 and C7 of the triazolo-fused triazine scaffold were modified to include a carbonyl, a thiocarbonyl and a thiomethyl groups, while the position C2 was modified by inserting different aromatic groups and longer flexible side chains. Moreover, compound endowed with promising TP inhibitory activity was tested to investigate its ability to suppress the MMP-9 expression, which has been reported to be upregulated by TP in breast cancer cells (25). In addition, a computational docking study was performed to determine potential site of binding and possible interactions of the synthesized compounds with the enzyme.

The synthesis of target compounds **IVa-IVo** and **IIa-IIb** was achieved by intramolecular heterocyclization of *N*-(1,2,4-triazol-5(3)-yl)-*N'*-carbethoxythioureas (**4**) and 5-amino-1-carbethoxylthiocarbamoyl-1,2,4-triazole (**5**), respectively, in an alkaline medium as illustrated in Scheme 1. The synthetic methods adopted here are based on the chemistry developed by Bokaldere and coworkers (26). This approach afforded products of high yields and purity. Compounds **IIIa-IIIb**, corresponding 7-methylthio derivatives of **IIa-IIb**, were prepared by treating **II** with iodomethane in aqueous alkali. This protocol afforded the products (**IIIa-IIIb**) with 61–67% yield. The resulting methylthio derivatives, **IIIa-IIIb**, were subsequently converted to compounds **Ia-Ib** *via* reaction of **IIIa-IIIb** with a mild oxidizing agent, hydrogen peroxide, in alkaline medium, and this reaction produced highly pure products with satisfactory yields (54–68%).

All the synthesized compounds were characterized by melting points and different spectroscopic techniques (^{1}H NMR, ^{13}C NMR and MS). The purity of the compounds was assessed by reverse-phase HPLC method and elemental analysis.[a] Interestingly, the structures of compounds **I–IV** were readily distinguished by the use of ^{13}C NMR spectroscopy. The ^{13}C peak of the thiocarbonyl (C = S) carbon of **IVb** appeared at around 175.8 ppm, while this group showed peaks at about 170.8 ppm for **IIb**. The appearance of the peak at about 11.8 ppm assigned to SMe in the ^{13}C NMR spectrum indicated the formation of product **IIIb**. The two signals of the carbonyl (C = O) groups of compound **IIa** appeared at about 152.5

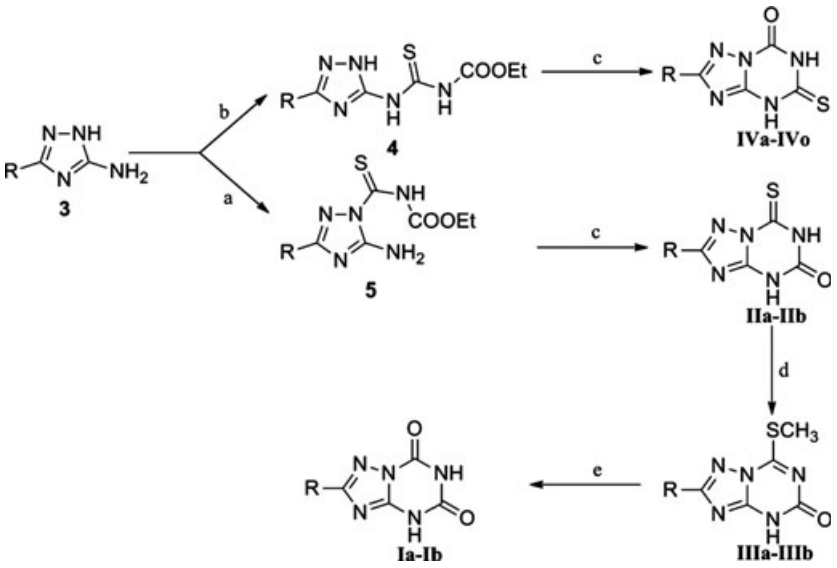

Scheme 1: Synthesis of target compounds (**I–IV**). Reagents and conditions: (A) Ethoxycarbonyl isothiocyanate, acetone, rt, 20 min (B) Ethoxycarbonyl isothiocyanate, DMF, rt, 4–5 h (C) NaOH, 80% ethanol (aq.), 100 °C, 20 min (D) MeI, NaOH, water, rt, 30 min (E) H_2O_2, NaOH, water, 60–70 °C, 4 h.

and 162.2 ppm in ^{13}C NMR spectra. The purity of all compounds was satisfactory (above 95%).

The four groups of compounds (**I, II, III and IV**) were evaluated for *in vitro* TP inhibitory activity by a spectrophotometric assay that used recombinant human thymidine phosphorylase, expressed in *E. coli* (T2807 – Sigma Aldrich). The original method developed by Krenitsky *et al.* (27) was modified and adopted. In this assay, the decrease in absorbance of thymidine (dThd) at 290 nm due to enzymatic reaction was monitored after 4, 8, 12, 16 and 20 min. Preliminary screening of enzyme inhibition was carried out at 100 μM of each compound. The inhibitory potency of each compound was calculated using GraphPad Prism version 4.0, and the results obtained were expressed in terms of IC_{50} values and were compared with that of **7-DX** (Table 1).

Unexpectedly, 1,2,4-triazolo[1,5-*a*][1,3,5]triazin-5,7-dione analogues **Ia** and **Ib** having the homophthalimide moiety did not display any inhibitory potential at 100 μM. This result was not consistent with the previous report, indicating that the homophthalimide group was a pharmacophoric requirement to impart inhibitory activity against TP (19). Modification of these compounds by replacing the oxygen atom at C7 with the bioisosteric sulfur resulted in no improvement in the activity. In addition, introduction of thiomethyl group at C7 and consequently removal of one active hydrogen at C6 in compounds **IIIa** and **IIIb** showed no activity, just like in the case of **IIa** and **IIb**. Interestingly, further modification of **IIa** and **IIb** by switching the positions of the carbonyl and thiocarbonyl moieties that afforded 5-thioxo-5,6-dihydro-4*H*-[1,2,4]triazole[1,5-a][1,3,5] triazin-7-one analogues (**IVa** and **IVb)** led to significant improvement in inhibition profile. Therefore, from the preliminary screening of different derivatives, it was revealed that a particular orientation of the C(=S)NHC(=O) moiety would be required to confer the inhibitory potency. Additional variation in substitution at C2 of **IVa** and **IVb** was carried out, and the resultant compounds **IVa-IVo** demonstrated varying degrees of TP inhibition with IC_{50} values ranging between 13 and 60 μM. The IC_{50} values of the test compounds were compared with the positive control, **7-DX**, that exhibited IC_{50} value of 42.63 μM in the same experimental conditions, which was found to be in accordance with the previous report (5). Compound **IVn**, 2-(4-bromo-3-methyl-phenyl)-5-thioxo-5,6-dihydro-4*H*-[1,2,4] triazolo[1,5-*a*][1,3,5]triazin-7-one, was observed to have best anti-TP activity (IC_{50} = 13.09 μM) among the four groups of compounds evaluated in this study. Compounds

Table 1: Thymidine phosphorylase inhibitory activity of the synthesized compounds (**I-IV**)

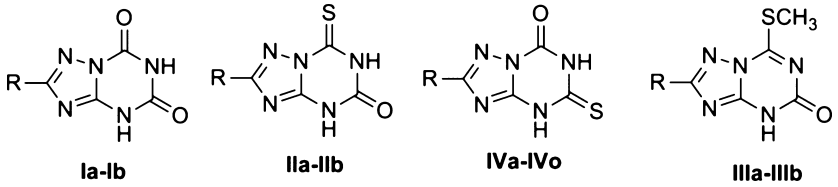

Entry	Compounds	R	Anti-TP activity[a] IC_{50} (μM)[b]
1	**Ia**	SCH_3	>100
2	**Ib**	Ph	>100
3	**IIa**	SCH_3	>100
4	**IIb**	Ph	>100
5	**IIIa**	SCH_3	>100
6	**IIIb**	Ph	>100
7	**IVa**	SCH_3	51.67 ± 5.92
8	**IVb**	Ph	39.56 ± 1.78
9	**IVc**	SCH_2Ph	55.38 ± 4.19
10	**IVd**	SCH_2CH_2Ph	59.88 ± 4.79
11	**IVe**	$SCH_2CH_2CH_2Ph$	59.25 ± 3.25
12	**IVf**	CH_2Ph	43.32 ± 5.03
13	**IVg**	2-furyl	31.54 ± 5.15
14	**IVh**	2-thienyl	30.95 ± 4.20
15	**IVi**	2-pyridyl	24.53 ± 4.91
16	**IVj**	4-MeC_6H_4	31.58 ± 3.10
17	**IVk**	4-BrC_6H_4	22.06 ± 4.42
18	**IVl**	3-MeC_6H_4	34.42 ± 3.21
19	**IVm**	3-BrC_6H_4	31.78 ± 3.56
20	**IVn**	4-Br,3-MeC_6H_3	13.09 ± 1.85
21	**IVo**	H	58.13 ± 2.61
22	**7-DX**	–	42.63 ± 5.25

[a]Values are means of three experiments.
[b]Values are presented as means ± SD.

IVa and **IVb** were also modified by inserting longer flexible side chain and higher spacer length at position C2; however, these efforts resulted in a decrease in activity, as evident in compounds **IVc**, **IVd**, **IVe** and **IVf**. In contrast, replacement of phenyl ring with other aromatic rings like furan, thiophene and pyridyl that yielded compounds **IVg**, **IVh** and **IVi** led to an improvement in binding affinity. In other words, the IC_{50} values of compounds **IVg**, **IVh** and **IVi** were 31.54 μM, 30.95 μM and 24.53 μM, respectively, that were lower to the IC_{50} value of **IVb**. The phenyl ring was modified by inserting electron-withdrawing (Br) and electron-donating (Me) substituents at both para- and meta-positions. Although a little difference in binding affinity was observed in metal-substituted compounds (**IVl** and **IVm**), compound **IVk** (logP – 2.29) having bromo-group at para-position displayed significantly higher activity compared with compound **IVj** (logP – 2.03) carrying methyl moiety. Therefore, it was evident that electronic effect of substitutions might have played a pivotal role in binding interactions. Moreover, it was believed that electron-withdrawing (Br) group may impart higher hydrophobicity to this compound, resulting in the enhancement of the TP inhibitory activity. As shown in the Table 1, with few exceptions, compounds (**IV**) with aromatic or aliphatic substituents at position C2 exhibited better inhibition profile than the unsubstituted compound **IVo,** which is considered as most structurally similar to the lead compound, **7-DX**.

Based on the results of TP inhibition analysis, we selected compound **IVn** for additional tests. To discriminate between reversible and irreversible inhibition, TP in a 1-mL reaction mixture (concentrations varying from 0.05 to 0.0075 U/mL) was treated with compound **IVn** at the concentration of 0 and 30 μM. The reaction mixture was incubated for 30 min at room temperature to monitor the conversion of dThd to thymine. The results of this experiment suggested that compound **IVn** behaved as a reversible inhibitor of the enzyme because two enzyme activity curves converge to the intersection (zero) point of the abscissa/ordinate graph (Figure 3). Reversible inhibitors bind to enzymes non-covalently, and the enzyme activity is recovered immediately after removal of the inhibitors and thus provide a potentially superior tolerability and safety profile as compared to irreversible inhibitors. Balzarini *et al.* and Hussain *et al.* (28,29) reported similar type of studies on the inhibition of TP with some TP inhibitors, belonging to diverse chemical classes. They also observed a similar inhibition type.

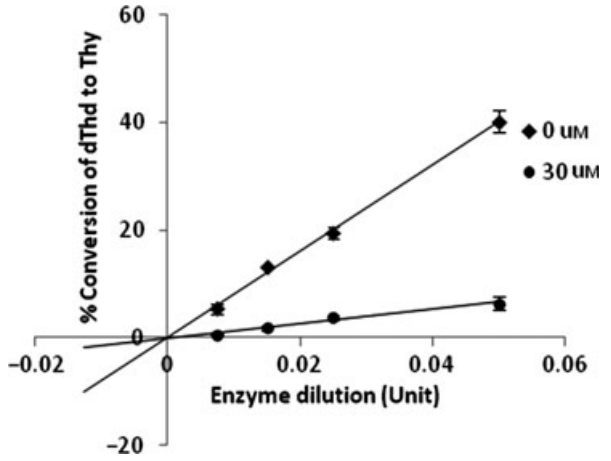

Figure 3: Reversible inhibition of TP by **IVn** was determined by incubating 0.05–0.0075 U/mL of TP in the presence of 30 μM of compound **IVn**. Control experiments were carried out using DMSO. Results are presented as means ± SD; SD denoted by error bars (Experiments carried out in triplicate).

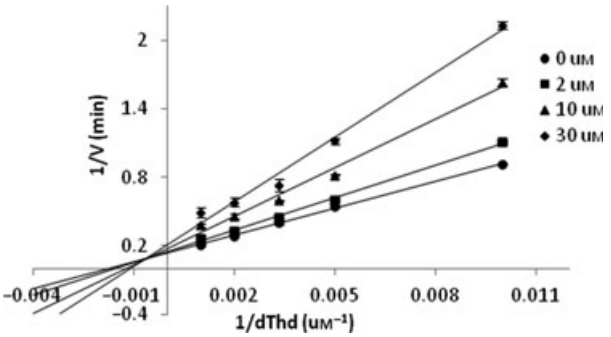

Figure 4: Lineweaver-Burk plots of TP inhibition by **IVn**, in the presence of variable concentrations of dThd demonstrating mixed type enzyme inhibition. Results are presented as means ± SD; SD denoted by error bars (Experiments carried out in triplicate).

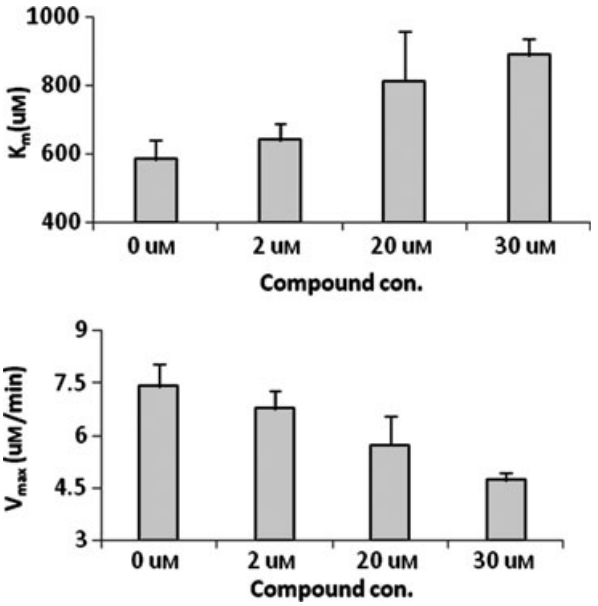

Figure 5: Response of kinetic parameters K_m and V_{max} with increasing concentration of **IVn** in variable concentrations of dThd. Results are presented as means ± SD; SD denoted by error bars (Experiments carried out in triplicate).

Table 2: A summary of the kinetic parameters of **IVn**

Compound	Substrate	K_i value (μM)[a,b]	α	Type of inhibition
IVn	dThd	24.21 ± 0.53	2.48	Mixed type

[a]Values are means of three experiments.
[b]Values are presented as means ± SD.

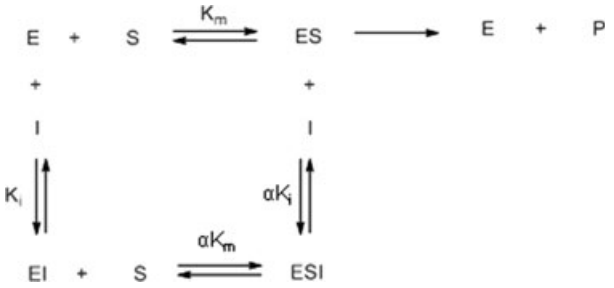

Scheme 2: Enzyme kinetic model for mixed type inhibition.

To elucidate the pattern of reversible inhibition, a brief kinetic study was attempted using compound **IVn** at different inhibitor concentrations (0, 2, 15, 20, 30 μM). The analysis was carried out by monitoring enzyme inhibition at varying thymidine (dThd) concentrations (1000, 500, 300, 200, 100 μM) and maintaining phosphate (KPi) concentration constant at 25 mM. The data obtained were analyzed by the double reciprocal plot method (Figure 4). The results implied that compound **IVn** was a mixed-type inhibitor in the presence of thymidine as a variable substrate because the straight lines corresponding to different concentrations of the inhibitor intersected in the second quadrant of the reciprocal plot. This was further confirmed by the fact that increasing inhibitor concentration was accompanied by an increase in K_m values, whereas the V_{max} values decreased gradually (Figure 5). Therefore, compound **IVn** can directly interact with enzyme as well as enzyme–substrate complex, which inactivates the enzyme but does not affect the binding of substrates. To explain the mixed-type inhibition, we adopted the model of Scheme 2. The inhibition constants (k_i and αK_i) for compound **IVn** were evaluated from replotting the slopes and intercepts of the double reciprocal plot against the inhibitor concentrations (Table 2). The values of inhibition constants (K_i and αK_i) (Table 2) indicated that the inhibitor has stronger affinity toward the free enzyme than enzyme–substrate complex ($\alpha > 1$). Moreover, the enzyme–inhibitor complex would exhibit lower affinity for substrate compared with free enzyme ($\alpha > 1$) (Scheme 2). These results suggested that compound **IVn** might interact with the enzyme differently compared with **7-DX**, which behaved as a competitive or mixed-type inhibitor in the presence of variable concentrations of thymine (28).

To investigate the ability of compound **IVn** to inhibit PMA-induced MNP-9 expression, gelatine zymography (30) was performed in MDA-MB-231 cells. The cells were treated with increasing doses of compound (50–200 μM) in the presence of PMA (80 nM). Interestingly, a decrease in band intensity compared with vehicle control was detected for compound **IVn** at 200 μM (Figure 6 A), indicating an attenuation of proteolytic activity of MMP-9 (band corresponded to the MW of 92 kDa) at the 200 μM concentration. Quantification of the band intensities in the zymograms using Image Gauge 4.0 software conferred that compound **IVn** significantly inhibited the MMP-9 activity at 100 and 200 μM concentrations ($p < 0.05$). The results also demonstrated that a PMA-induced increase in MMP-9 expression

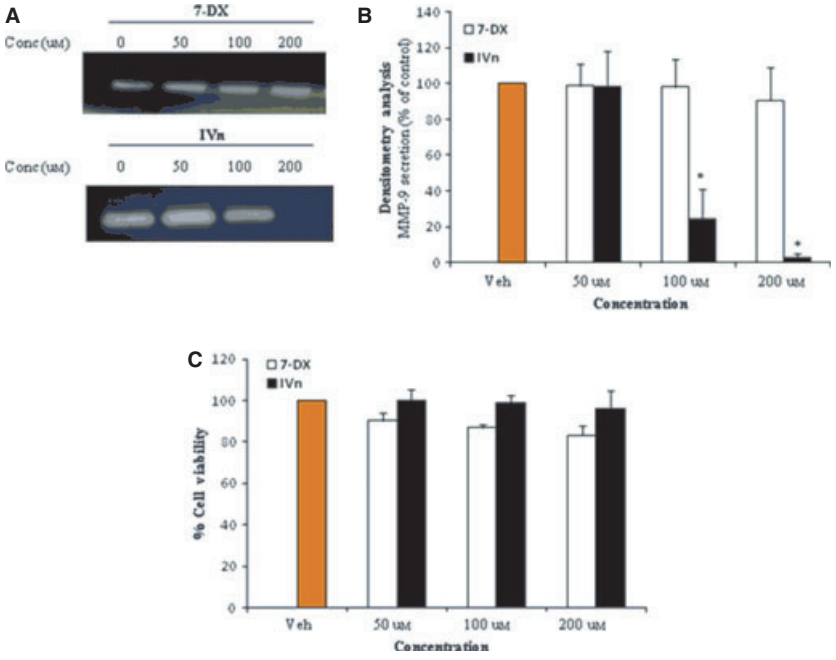

Figure 6: Effect of compound **IVn** and **7-DX** on PMA-induced MMP-9 expression and cell growth in MDA-MB-231 cells: (A) suppressive effects of **IVn** and **7-DX** on MMP-9 expression and their dose response; (B) densitometry analysis of MMP-9 expression. (C) cell viability (%) of cells after 72 h treatment of compound **IVn** and **7-DX**. Results are presented as means ± SD; SD denoted by error bars (Experiments carried out in triplicate). *$p < 0.05$.

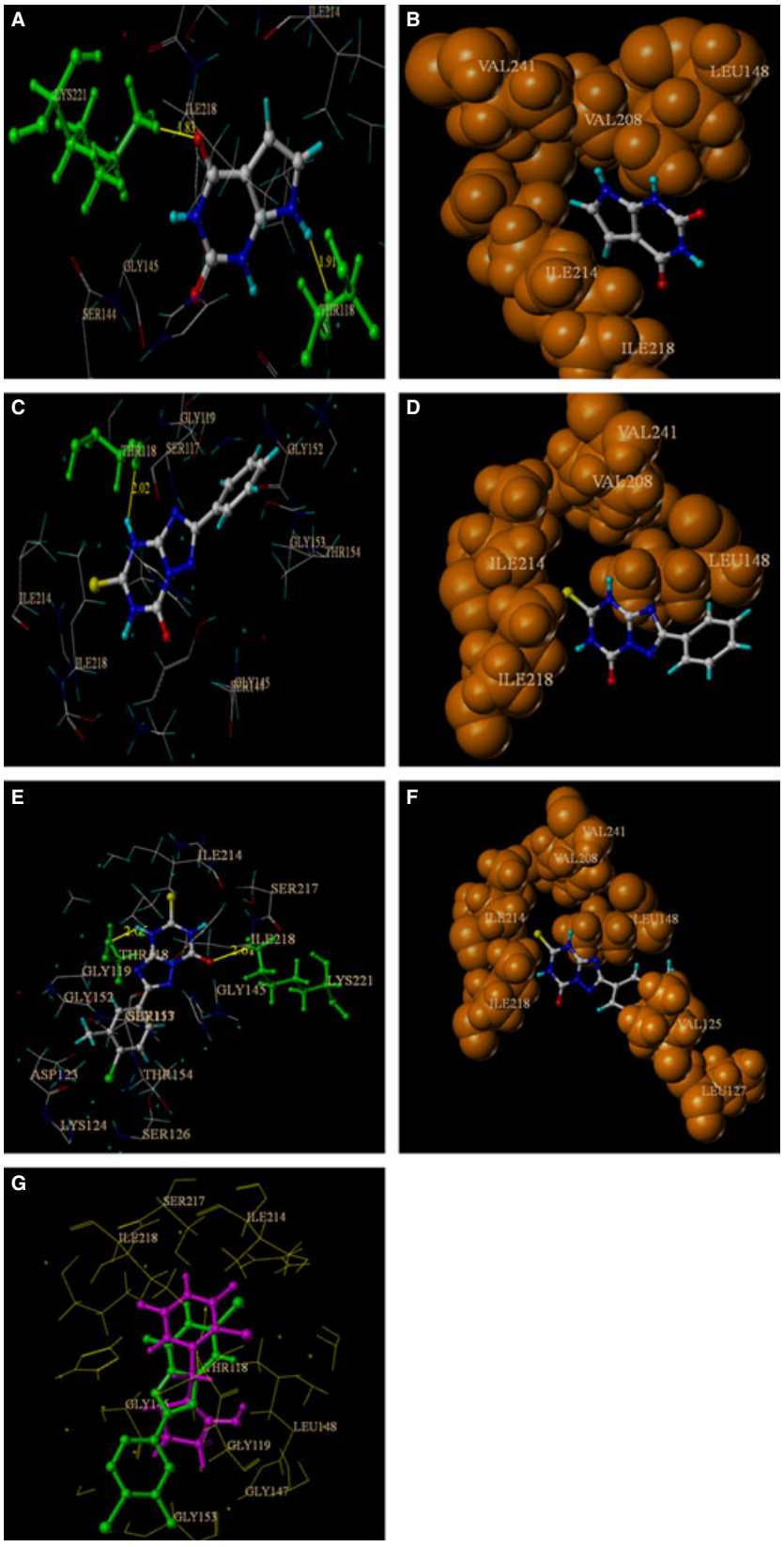

Figure 7: Graphical representation of interactions between TP and its inhibitors analyzed by computational docking: (A) hydrogen bonding of **7-DX** (colored ball and stick) with Lys221, Thr118 (green colored ball and stick); (B) hydrophobic interaction of **7-DX** (colored ball and stick) with amino acid (orange colored sphere); (C) hydrogen bonding of **IVb** (colored ball and stick) with Thr118 (green colored ball and stick); (D) hydrophobic interaction of **IVb** (colored ball and stick) with amino acid (orange colored sphere); (E) hydrogen bonding of **IVn** (colored ball and stick) with Lys221 and Thr118 (green colored ball and stick); (F) hydrophobic interaction of **IVn** (colored ball and stick) with amino acid (orange colored sphere); (G) an overlay of **TPI** and **IVn** bound to the active site of TP (**TPI**, in pink and **IVn,** in green).

was suppressed dose dependently by the compound **IVn** (Figure 6 B). However, reference inhibitor, **7-DX**, did not display any substantial inhibition of MMP-9 secretion even at the 200 μM concentration.

To ascertain that the inhibition of MMP-9 expression by the compound was not the consequence of its cytotoxic effect, the inhibitory effect of the test compounds on MDA-MB-231 cell growth was determined by means of MTT assay (31). As depicted in Figure 5 C, compounds **IVn** and **7-DX** exhibited cell viability at around 80–100% at the tested doses after 72 h of exposure as compared to vehicle control (Figure 6 C).

To explore the plausible binding mode and molecular interactions responsible for enzyme inhibition of the synthesized compounds, geometry-optimized structure of compounds was allowed to dock at the active site of TP (PDB code: 2WK6) (32) using SYBYL-X 1.3. The lowest energy conformation of the compounds was adopted to analyze the docking results. Before docking, the docking protocol was validated by comparing the binding interaction of **TPI** in the active site of TP with the previously reported results. The predicted binding mode and interaction pattern of **TPI** generated by our software were closely matching with the reported crystallographic study (33) with a RMS deviation of 0.5 Å (Figure S1 a, b in Appendix S1).

The analysis of molecular docking between TP and reference compound, **7-DX,** suggested that the carbonyl group at C4 and NH-7 of **7-DX** formed strong hydrogen-bonding contacts with Lys221 and Tyr118, respectively, located in the active site of enzyme (33) (Figure 7 A). The NH group adjacent to the thiocarbonyl moiety in identified inhibitor (**IVb**) demonstrated hydrogen-bonding interaction with Tyr118, whereas the thiocarbonyl moiety placed itself into a hydrophobic space created by some amino acid residues like Ile-218, Ile-214, Val-208, Val-241, Val-208 and Leu-148 (Figure 7 C, D). As a result, the compound **IVb** exhibited inhibitory activity with an IC_{50} value in micromolar range being comparable with **7-DX** (Table 1). On the other hand, compounds **Ib, IIb** and **IIIb** were found to be inactive, although they displayed the higher total score compared with **IVb** (Table 3). The compound **Ib** could not produce tight hydrophobic contact into the hydrophobic pocket as compared to compound **IVb** due to the presence of carbonyl moiety at C5 that has smaller atomic size as well as high polarity, which led to misalignment of the entire compound (Figure S1 c, d in Appendix S1). More-

Table 3: Comparison of docking scores (kcal/mol) of compounds (**I–IV**)

Cpd	Total Score[a]	Crash Score[b]	Polar Score[c]	G Score[d]	PMF Score[e]	D Score[f]	Chem Score[g]	C Score[h]
Ia	4.43	−0.92	1.14	96.08	135.53	−8.47	-3.20	1
Ib	4.75	−1.22	1.72	101.44	143.96	−13.14	−6.38	1
IIa	4.57	−0.76	1.11	96.08	122.07	−18.89	−3.18	1
IIb	3.98	−2.71	1.18	95.31	120.39	−20.01	−6.28	2
IIIa	4.61	−2.33	1.61	88.66	138.93	−21.65	−3.33	1
IIIb	3.75	−3.63	1.57	87.70	136.40	−22.57	−4.72	1
IVa	2.93	−0.51	1.10	86.51	122.02	−17.13	−3.49	1
IVb	3.46	−1.07	0.83	83.74	93.10	−15.30	−8.22	3
IVc	3.96	−2.97	1.36	102.97	134.32	−11.05	−3.34	0
IVd	3.46	−3.65	0.76	89.55	137.87	−9.87	−3.42	0
IVe	3.04	−5.23	1.02	97.43	134.68	−11.02	−3.63	0
IVf	4.48	−1.45	0.64	72.01	110.27	−14.03	−7.27	2
IVg	2.17	−1.50	0.28	54.70	73.54	−10.97	−6.95	2
IVh	2.41	−1.64	0.34	70.15	60.23	−11.25	−6.12	2
IVi	2.85	−0.99	0.72	80.92	92.26	−14.90	−8.32	3
IVj	3.48	−1.99	0.64	84.70	115.63	−14.62	−5.99	2
IVk	2.39	−1.84	2.03	58.17	63.30	−13.18	−7.83	3
IVl	4.24	−1.85	0.79	82.98	93.96	−14.17	−8.12	2
IVm	3.09	−1.76	0.62	70.74	95.68	−11.47	−8.10	3
IVn	3.19	−1.87	0.85	83.45	102.24	−15.50	−5.91	3
IVo	3.73	−0.63	1.13	98.63	126.32	−6.58	−5.52	0
7-DX	4.98	−0.66	2.16	108.26	142.09	−8.52	−8.25	1

[a]Total score reports total output of all the scores.
[b]Crash score indicating the ability of the compound to penetrate the active site of the protein.
[c]Polar score showing the polar interaction between the ligand and the protein.
[d]G score revealing hydrogen bonding, complex (ligand-protein) and internal (ligand–ligand) interaction.
[e]MF score demonstrates the free energies of interactions for protein–ligand atom pairs.
[f]D score is based on van der Waals interaction between protein and ligand.
[g]Chem score includes terms for hydrogen bonding, metal–ligand interaction, lipophilic contact and rotational entropy, along with an intercept term.
[h]C score: the consensus score: It exhibits the sum of the number of 'good' results for each ligand in each scoring function.

over, the energy required for hydrogen bonding, metal–ligand interaction, lipophilic contact and rotational entropy for **IVb** is less compared with **Ib** that is reflected in their G score, PMF score, D score and Chem score (Table 3). The compounds **IIb** and **IIIb** were having inappropriate penetration (Crash score −2.71, −3.63 kcal/mol, respectively) into the binding site, resulting in a decrease in interaction forces with the amino acids of binding site. A similar trend was observed for compounds bearing thiomethyl moiety (**Ia**, **IIa**, **IIIa**, **IVa**) (Table 3).

It was also evident from the docking score (Table 3) that insertion of flexible chains into the lead structure (**IVb**) resulted in inappropriate penetration and diminished inhibitory potential, as found in compounds **IVc**, **IVd**, **IVe** and **IVf** (Crash score −2.97, −3.65, −5.23, and −1.45 kcal/mol, respectively). The total score, D score, Chem score are in favor of compound **IVi,** and thus, it exhibited higher inhibitory response (IC_{50} = 24.53 μM) among all other heterocyclic derivatives (**IVg**, **IVh** and **IVi**). The most active compound **IVn** showed an improvement in interactions with respect to hydrogen bond formation and hydrophobic contacts compared with compound **IVb** (Figure 7 E,F). Moreover, compound **IVn** exhibited better polar interaction, hydrogen bonding, complex (ligand–protein) and internal (ligand–ligand) energies, free energies of interactions and van der Waals interaction than positive control, **7-DX** (Table 3). The analysis of molecular docking between TP and **IVn** suggested that although compound **IVn** interacted with amino acid residues located at or adjacent to the thymidine binding site (33), the binding orientation of **IVn** was different compared with **TPI** (competitive inhibitor), and consequently, it showed a mixed-type inhibition with respect to thymidine (Figure 7 G).

In conclusion, the intramolecular heterocyclization reaction was used to generate the target 1,2,4-triazolo[1,5-*a*][1,3,5] triazine derivatives. The *in vitro* evaluation of anti-TP effect revealed that among the different derivatives of 1,2,4-triazolo[1,5-*a*][1,3,5]triazine, compounds having thiocarbonyl group and carbonyl group in positions C5 and C7, respectively, *viz.,* 5-thioxo-5,6-dihydro-4*H*-[1,2,4]triazolo[1,5-*a*] [1,3,5]triazin-7-one and its analogues, showed inhibitory activity against TP. The representative compound **IVn** was found to exhibit mixed-type inhibition toward the enzyme in the presence of variable concentrations of thymidine, which was consistent with the results derived from the molecular docking experiment. Compound **IVn** also inhibited MMP-9 expression in MDA-MB-231 cells at sublethal concentrations. Moreover, the docking study gave a justified binding mode of the active as well as inactive compounds in the binding site of TP. Therefore, these compounds would serve as leads for further design and optimization of fused-ring TP inhibitors. Following these promising results, further studies are in progress with diverse structural modifications on that scaffolds for improved biological activities, and the results obtained from these efforts and structure–activity relationships will be reported in the due course.

Acknowledgments

The authors are thankful to the National Medical Research Council grant, Singapore (R-148-000-102-275), and Academic Research Funds of National University of Singapore for their financial assistance. Thanks are also extended to Gokaraju Rangaraju Educational Society for providing essential laboratory facilities and support for this project. There are no conflict of interests to be mentioned.

References

1. Asai K., Nakanishi K., Isobe I., Eksioglu Y.Z., Hirano A., Hama K., Miyamoto T., Kato T. (1992) Neurotrophic action of gliostatin on cortical neurons. Identity of gliostatin and platelet-derived endothelial cell growth factor. J Biol Chem;267:20311–20316.
2. Iltzsch M.H., El Kouni M.H., Cha S. (1985) Kinetic studies of thymidine phosphorylase from mouse liver. Biochemistry;24:6799–6807.
3. Schwartz M. (1971) Thymidine phosphorylase from Escherichia coli. Properties and kinetics. Eur J Biochem;21:191–198.
4. Takebayashi Y., Yamada K., Miyadera K., Sumizawa T., Furukawa T., Kinoshita F., Aoki D., Okumura H., Yamada Y., Akiyama S., Aikou T. (1996) The activity and expression of thymidine phosphorylase in human solid tumours. Eur J Cancer; Pt A32:1227–1232.
5. Pocher F., Spadari S. (2001) Thymidine phosphorylase: a two-face Janus in anticancer chemotherapy. Curr Cancer Drug Targets;1:141–153.
6. Perez-Perez M.J., Priego E.M., Hernandez A.I., Camarasa M.J., Balzarini J., Liekens S. (2005) Thymidine phosphorylase inhibitors: recent developments and potential therapeutic applications. Mini Rev Med Chem;5:1113–1123.
7. Brown N.S., Jones A., Fujiyama C., Harris A.L., Bicknell R. (2000) Thymidine phosphorylase induces carcinoma cell oxidative stress and promotes secretion of angiogenic factors. Cancer Res;60:6298–6302.
8. Gunningham S.P., Currie M.J., Morrin H.R., Tan E.Y., Turley H., Dachs G.U., Watson A.I., Frampton C., Robinson B.A., Fox S.B. (2007) The angiogenic factor thymidine phosphorylase up-regulates the cell adhesion molecule P-selectin in human vascular endothelial cells and is associated with P-selectin expression in breast cancers. J Pathol;212:335–344.
9. Muro H., Waguri-Nagaya Y., Mukofujiwara Y., Iwahashi T., Otsuka T., Matsui N., Moriyama A., Asai K., Kato T. (1999) Autocrine induction of gliostatin/platelet-derived endothelial cell growth factor (GLS/PD-ECGF) and GLS-induced expression of matrix metalloproteinases

in rheumatoid arthritis synoviocytes. Rheumatology 38: 1195–1202.
10. Pula G., Mayr U., Evans C., Prokopi M., Vara D.S., Yin X., Astroulakis Z., Xiao Q., Hill J., Xu Q., Mayr M. (2009) Proteomics identifies thymidine phosphorylase as a key regulator of the angiogenic potential of colony forming units and endothelial progenitor cell cultures. Circ Res;104:32–40.
11. Bijnsdorp I.V., Capriotti F., Kruyt F.A.E., Losekoot N., Fukushima M., Griffioen A.W., Thijssen V.L., Peters G.J. (2011) Thymidine phosphorylase in cancer cells stimulates human endothelial cell migration and invasion by the secretion of angiogenic factors. Br J Cancer;104:1185–1192.
12. Ikeda R., Furukawa T., Mitsuo R., Noguchi T., Kitazono M., Okumura H., Sumizawa T., *et al.* (2003) Thymidine phosphorylase inhibits apoptosis induced by cisplatin. Biochem Biophys Res Commun;301:358–363.
13. Kitazono M., Takebayashi Y., Ishitsuka K., Takao S., Tani A., Furukawa T., Miyadera K., Yamada Y., Aikou T., Akiyama S. (1998) Prevention of hypoxia-induced apoptosis by the angiogenic factor thymidine phosphorylase. Biochem Biophys Res Commun;253:797–803.
14. Rofstad E.K., Halsor E.F. (2000) Vascular endothelial growth factor, interleukin 8, platelet-derived endothelial cell growth factor, and basic fibroblast growth factor promote angiogenesis and metastasis in human melanoma xenografts. Cancer Res;60:4932–4938.
15. Bronckaers A., Gago F., Balzarini J., Liekens S. (2009) The dual role of thymidine phosphorylase in cancer development and chemotherapy. Med Res Rev;29:903–953.
16. Yano S., Kazuno H., Suzuki N., Emura T., Wierzba K., Yamashita J.I., Tada Y., Yamada Y., Fukushima M., Asao T. (2004) Synthesis and evaluation of 6-methylene-bridged uracil derivatives. Part 1: discovery of novel orally active inhibitors of human thymidine phosphorylase. Bioorg Med Chem;12:3431–3441.
17. Diab S.A., De Schutter C., Muzard M., Plantier-Royon R., Pfund E., Lequeux T. (2012) Fluorophosphonylated nucleoside derivatives as new series of thymidine phosphorylase multisubstrate inhibitors. J Med Chem 55: 2758–2768.
18. Pomeisl K., Horska K., Pohl R., Blažek J., Krečmerova M. (2012) Syntheses of 1-[2 (phosphonomethoxy)alkyl]thymine monophosphates and an evaluation of their inhibitory activity toward human thymidine phosphorylase. Nucleosides, Nucleotides Nucleic Acids;31:159–171.
19. Baker B.R., Kelley J.L. (1970) Irreversible enzyme inhibitors. CLXXI. Inhibition of FUDR phosphorylase from Walker 256 rat tumor by 5-substituted uracils. J Med Chem;13:461–466.
20. Fukushima M., Suzuki N., Emura T., Yano S., Kazuno H., Tada Y., Yamada Y., Asao T. (2000) Structure and activity of specific inhibitors of thymidine phosphorylase to potentiate the function of antitumor 2'-deoxyribonucleosides. Biochem Pharmacol;59:1227–1236.
21. Poucher S.M., Keddie J.R., Brooks R., Shaw G.R., McKillop D. (1996) Pharmacodynamics of ZM 241385, a potent A(2a) adenosine receptor antagonist, after enteric administration in rat, cat and dog. J Pharm Pharmacol;48:601–606.
22. Keddie J.R., Poucher S.M., Shaw G.R., Brooks R., Collis M.G. (1996) In vivo characterisation of ZM 241385, a selective adenosine A2A receptor antagonist. Eur J Pharmacol;301:107–113.
23. Robins R.K., Revankar G.R., O'Brien D.E. (1985) Purine analog inhibitors of xanthine oxidase - Structure activity relationships and proposed binding of the molybdenum cofactor. J Heterocycl Chem;22:601–634.
24. Dolzhenko A.V., Dolzhenko A.V., Chui W.K. (2006) 1,2,4-triazolo[1,5- *a*][1,3,5]triazines (5-azapurines): synthesis and biological activity. Heterocycles;68:1723–1759.
25. Kurizaki T., Toi M., Tominaga T. (1998) Relationship between matrix metalloproteinase expression and tumor angiogenesis in human breast carcinoma. Oncol Rep;5:673–677.
26. Bokaldere R., Liepina A. (1973) s-Triazolo[1,5-*a*]-s-triazinonethiones. Synthesis and reactions. Khim Geterotsikl Soedin;2:276–280.
27. Krenitsky T.A., Bushby S.R.M. (1979) U.S. Patent, 4, 178,212, 1-8, Research Triangle Park, NC: Burroughs Welcome Co., 1979.
28. Balzarini J., Degreve B., Esteban-Gamboa A., Esnouf R., De Clercq E., Engelborghs Y., Camarasa M.J., Pérez-Pérez M.J. (2000) Kinetic analysis of novel multisubstrate analogue inhibitors of thymidine phosphorylase. FEBS Lett;483:181–185.
29. Hussain S., Gaffney J., Ahmed N., Slevin M., Iqbal Choudhary M., Ahmad V.U., Qasmi Z., Abbasi M.A. (2009) An investigation of the kinetic and anti-angiogenic properties of plant glycoside inhibitors of thymidine phosphorylase. J Asian Nat Prod Res;11:159–167.
30. Liotta L.A., Stetler-Stevenson W.G. (1990) Metalloproteinases and cancer invasion. Semin Cancer Biol;1:99–106.
31. Alley M.C., Scudiero D.A., Monks A., Hursey Czerwinski M.L.M.J., Fine D.L., Abbott B.J., Mayo J.G., Shoemaker R.H., Boyd M.R. (1988) Feasibility of drug screening with panels of human tumor cell lines using a microculture tetrazolium assay. Cancer Res;48:589–601.
32. Mitsiki E., Papageorgiou A.C., Iyer S., Thiyagarajan N., Prior S.H., Sleep D., Finnis C., Acharya K.R. (2009) Structures of native human thymidine phosphorylase and in complex with 5- iodouracil. Biochem Biophys Res Commun;386:666–670.
33. Norman R.A., Barry S.T., Bate M., Breed J., Colls J.G., Ernill R.J., Luke R.W., Minshull C.A., McAlister M.S., McCall E.J., McMiken H.H., Paterson D.S., Timms D., Tucker J.A., Pauptit R.A. (2004) Crystal Structure of Human Thymidine Phosphorylase in

Complex with a Small Molecule Inhibitor. Structure;12:75–84.

Note

[a]All final compounds were characterized by 1H NMR, 13C NMR, ESI-MS and elemental analysis. Representative examples, 2-phenyl-5-thioxo-5,6-dihydro-4H-[1,2,4]triazolo [1,5-a][1,3,5]triazin-7-one (IVb). Yield 78%; mp 258–259 °C (EtOH); ESI-MS m/z 244.1 (M-1)+; purity > 95%; 1H NMR (300 MHz, DMSO-d6): δ 7.53–7.55 (m, 3H, H-3', H-4' and H-5'), 8.04–8.07 (m, 2H, H-2' and H-6'), 13.12 (s, 1H, NH), 14.31 (br. s, 1H, NH); 13C NMR (75 MHz, DMSO-d6): δ 127.1 (C-2' and C-6'), 129.5 (C-3' and C-5'), 129.7 (C-4'), 131.3 (C-1'), 141.7 (C-2), 151.9 (C-9), 162.4 (C-7), 175.8 (C-5); Anal. calcd. for C10H7N5OS: C, 48.97; H, 2.88; N, 28.55. Found: C, 48.28; H, 2.71; N, 28.20.

Supporting Information

Additional Supporting Information may be found in the online version of this article:

Appendix S1. Full experimental detail, ^{1}H and ^{13}C NMR spectra.

Figure S1. Molecular interactions of **TPI** and **Ib** with enzyme, thymidine phosphorylase: (a) hydrogen bonding of **TPI** (colored ball and stick) with Ser217, Arg202, Lys221, Thr151 and His116 (green colored ball and stick); (b) hydrophobic interaction of **TPI** (colored ball and stick) with amino acid (orange colored sphere); (c) hydrogen bonding of **Ib** (colored ball and stick) with Ser217, Arg202 and Lys221 (green colored ball and stick); (d) hydrophobic interaction of **Ib** (colored ball and stick) with amino acid (orange colored sphere).